ACS APPLIED MATERIALS & INTERFACES

Research Article

www.acsami.org

Ce-Doped YAG Nanophosphor and Red Emitting $CuInS_2$/ZnS Core/Shell Quantum Dots for Warm White Light-Emitting Diode with High Color Rendering Index

Abdelhay Aboulaich,[*,†] Martyna Michalska,[‡] Raphaël Schneider,[§] Audrey Potdevin,[∥,⊥] Jérôme Deschamps,[†] Rodolphe Deloncle,[†] Geneviève Chadeyron,[∥,⊥] and Rachid Mahiou[†,∥]

[†]Clermont Université, Université Blaise Pascal, Institut de Chimie de Clermont-Ferrand, 24 Avenue des Landais, BP 80026, 63174, Aubière, France

[‡]NanoBioMedical Centre and Department of Macromolecular Physics, Adam Mickiewicz University, Umultowska 85, 61-614 Poznan, Poland

[§]Laboratoire Réactions et Génie des Procédés (LRGP), UMR 7274, Université de Lorraine, CNRS, 1 rue Grandville, BP 20451, 54001 Nancy Cedex, France

[∥]CNRS, UMR 6296, ICCF, BP 80026, 63171, Aubière, France

[⊥]Clermont Université, ENSCCF, Institut de Chimie de Clermont-Ferrand, BP 10448, 63000 Clermont-Ferrand, France

Supporting Information

ABSTRACT: In this work, we report the solvothermal synthesis of Ce-doped YAG (YAG:Ce) nanoparticles (NPs) and their association with a free-Cd $CuInS_2$/ZnS (CIS/ZnS) core/shell QDs for application into white light emitting diode (WLED). 1500 °C-annealed YAG:Ce NPs and CIS/ZnS core/shell QDs exhibited intense yellow and red emissions band with maxima at 545 and 667 nm, respectively. Both YAG:Ce nanophosphor and CIS/ZnS QDs showed high photoluminescence quantum yield (PL QY) of about 50% upon 460 nm excitation. YAG:Ce nanophosphor layer and bilayered YAG:Ce nanophosphor-CIS/ZnS QDs were applied on blue InGaN chip as converter wavelength to achieve WLED. While YAG:Ce nanophosphor converter layer showed low color rendering index (CRI) and cold white light, bilayered YAG:Ce nanophosphor-CIS/ZnS QDs displayed higher CRI of about 84 and warm white light with a correlated color temperature (CCT) of 2784 K. WLED characteristics were measured as a function of forward current from 20 to 1200 mA. The white light stability of bilayered nanophosphor-QDs-based WLED operated at 200 mA was also studied as a function of operating time up to 40 h. Interestingly, CRI and CCT of such device tend to remain constant after 7 h of operating time suggesting that layer-by-layer structure of YAG:Ce phosphor and red-emitting CIS/ZnS QDs could be a good solution to achieve stable warm WLED, especially when high current density is applied.

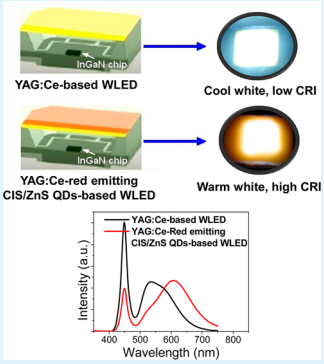

KEYWORDS: *$CuInS_2$/ZnS core/shell QDs, YAG:Ce-CIS/ZnS QDs/silicone film, bilayered structure, white LED*

INTRODUCTION

Phosphor-converted white light-emitting diode (pc-WLEDs) have received considerable attention because of their potential applications in solid-state lightings and display systems.[1] The wide interest in pc-WLEDs arises from their unique properties including low power consumption, environmental friendliness, small volume, long lifetime, and many more, making these devices very promising candidates to replace currently used incandescent and fluorescent lamps.[2−5] Typical pc-WLED consists of a 460 nm InGaN blue LED chip and Ce-doped yttrium aluminum garnet (YAG:Ce) phosphor, which efficiently converts a blue light from LED into a very broad yellow emission band, generating a white light by the combination of blue and yellow lights.[6,7] YAG:Ce-based WLEDs possess many advantages compared to other WLEDs systems as easy fabrication and low cost. However, the light from YAG:Ce-based WLEDs is colder and bluer than that from conventional incandescent and fluorescent devices. Indeed, YAG:Ce/blue LED system has a poor color rendering index (CRI) because of the red-deficiency of YAG:Ce phosphor, which hinders the development of WLEDs with high CRI (>80) and low correlated color temperature (CCT). To overcome these problems, two approaches have been proposed in the literature. One consists in the modification of its chemical composition either (i) by codoping using rare earth ions that can emit red emission, such as Cr^{3+}, Pr^{3+}, Sm^{3+}, and Mn^{2+},[8−12] or (ii) by substituting Al^{3+} and Y^{3+} in $Y_3Al_5O_{12}$ structure by other cations, such as Tb^{3+}, Gd^{3+}, and Mg^{2+},[8,13,14] and finally (iii) by replacing O^{2-} anions by ligands with a lower electronegativity such as N^{3-} with Si^{4+} charge compensation.[5]

Received: September 21, 2013
Accepted: December 9, 2013
Published: December 9, 2013

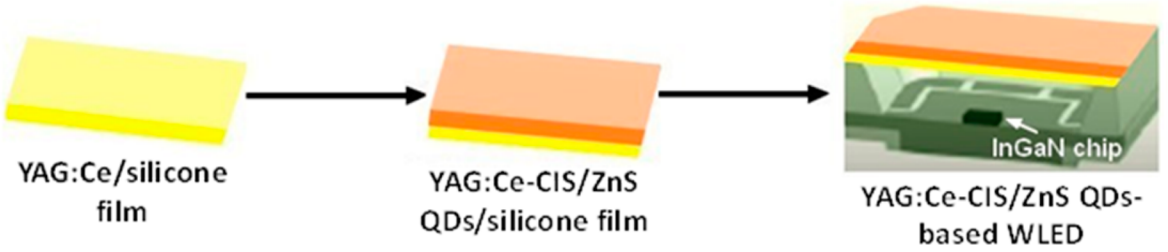

Figure 1. Schematic of fabrication of YAG:Ce-CIS/ZnS QD-based WLED Device.

This way successfully leads to YAG:Ce emission spectrum shift to longer wavelengths but unfortunately causes noticeable decrease in emission intensity and luminous efficiency of pc-WLEDs while the Ce^{3+} emission red-shift is limited.[15] The second method consists in mixing YAG:Ce phosphor with red or orange-emitting phosphors including nitrides, oxynitrides phosphors, such as Eu^{2+}-doped $M_2Si_5N_8$ (M = Ca, Sr or Ba), $MAlSiN_3$, and $MSi_2O_2N_2$ (M = Ca or Sr), and sulfides phosphors, such as Eu^{2+}-doped CaS, SrS, and (Sr,Ca)S.[16] Although this method has been widely adopted to achieve warm WLED, moisture instability of sulfide, and high reaction temperature (over 1800 °C) and pressure of nitride phosphors are critical problems.[15] Currently, the development of semiconductor nanocrystals, so-called quantum dots (QDs), as wavelength converter materials for WLEDs is widely under progress.[17,18] The growing interest of QDs in solid state lighting technology lies in the fact that these emitters have many advantages compared to conventional micro-sized ceramic phosphors, for examples, tunable emission by simply altering the nanocrystal size or composition, very narrow band emission, saturated color, high quantum efficiency (QE), and non-scattering properties because of their small size.[19−21] Recently, significant progress has also been made toward large-scale synthesis of this class of luminescent nanomaterials.[22,23] Among them, Cd-free QDs are attracting more and more attention from scientists and lighting devices manufacturers mainly because of their low toxicity compared to Cd-based ones such as CdSe, CdTe, and CdS QDs. It especially includes core/shell QDs such as InP/ZnS, doped core/shell QDs, such as ZnSe:Mn/ZnS, and alloy core−shell QDs, such as $CuInS_2$/ZnS (CIS/ZnS).[23−27] Combined with a blue or near-UV LED chip, CIS/ZnS QDs with various Cu/In ratios have been used as wavelength-converters to make QDs-WLEDs. For instance, highly luminous efficiency of 63.4 lm W^{-1} and CRI of 72 were reported when yellow-emitting CIS/ZnS core/shell QDs (Cu/In = 1/4) were combined with blue LED chip at a forward current of 20 mA.[23] Orange-emitting CIS/ZnS QDs with a peak wavelength at 570 nm have also been used to correct red-deficiency of YAG:Ce phosphor.[28] Zou and co-workers also randomly mixed red-emitting CIS/ZnS QDs with commercial yellow emissive YAG:Ce and green emissive Eu^{2+}-doped silicate phosphors to achieve warm white LED.[29] Despite the successful application of CIS/ZnS QDs as wavelength converters in low power LEDs, little attention was paid so far to the stability overtime of such nanomaterials in WLED especially when high forward current (≥200 mA) is applied. This is partly because of high temperature-dependence of the luminescence of CIS/ZnS QDs. Besides, YAG:Ce phosphor is conventionally synthesized at high temperature via a solid-state reaction process or other high temperature methods under H_2 reducing atmosphere to prevent Ce^{3+} from oxidation thus requiring expensive and complicated process. In this study, we synthesized YAG:Ce nanophosphor via solvothermal method according to our previous report.[30] To achieve highly crystalline and efficient garnet phosphor, solvothermally synthesized YAG:Ce nanoparticles (NPs) were annealed at 1500 °C without H_2 reducing flux. Otherwise, phosphor arrangement and geometry are one of the key parameters toward high light extraction, high lifetime and better color control in WLE devices.[31,32] For instance, You et al. reported that bilayered red/yellow phosphors configuration had higher luminous flux, higher phosphor conversion efficiency and lower junction-temperature compared to conventional random mixed phosphor case at the same CCT.[33] Indeed, separate red and yellow phosphors considerably lead to low back reflection of light inside the WLED package. In this work, YAG:Ce phosphor and CIS/ZnS core−shell QDs were separately dispersed in silicone resin and piled up as red/yellow bilayered luminescent film as shown in Figure 1. The resulting YAG:Ce-CIS/ZnS QDs bilayered structure was then combined with blue LED to achieve warm WLED having high CRI (>80).

EXPERIMENTAL SECTION

Synthesis of Ce-Doped YAG Phosphor. YAG:Ce phosphor was prepared from yttrium and cerium acetate mixed with aluminum isopropoxide in a glycol solvents according to a solvothermal method already detailed in our previous report.[30] The as-synthesized YAG:Ce suspension was dried at 80 °C. The dried pale-yellow powder was then annealed at 1500 °C in a muffle furnace for 4 h. A bright yellow phosphor powder was obtained.

Synthesis of CIS/ZnS Core/Shell QDs. *CIS Core Synthesis.* In a typical synthesis, 0.14 mmol of CuI and 0.2 mmol of $In(OAc)_3$ were dispersed in 50 mmol octadecene into a three-neck flask under argon flow. The flask was next degassed for 20 min under vacuum at 75 °C to remove water and oxygen traces. Dodecanethiol (8.3 mmol) were then injected, and the temperature was raised to 210 °C. The reaction time was fixed at 20 min.

Core/Shell CIS/ZnS Synthesis. To the crude CIS QDs obtained after 20 min heating, 0.4 mmol of anhydrous zinc acetate and 4.2 mmol of oleylamine were added. The temperature was next increased to 220 °C and the mixture maintained at that temperature for 2.5 h. The reaction flask was then cooled down to room temperature. The resulting CIS/ZnS QDs were precipitated with an excess of ethanol, purified repeatedly with a solvent combination of chloroform/ethanol by centrifugation and dried under vacuum for 12 h.

Preparation of YAG:Ce/Silicone and YAG:Ce-CIS/ZnS QDs/Silicone Films. To conduct a comparative study, we separately prepared YAG:Ce/silicone and YAG:Ce-CIS/ZnS QDs/silicone films.

Preparation of YAG:Ce/Silicone Film. YAG:Ce/silicone mixture was prepared by dispersing 0.68 g of YAG:Ce phosphor in 6 g of silicone resin/curing agent (Gelest OE (TM) 41, 2-part Silicone RTV Encapsulant PP2-OE41, ABCR), the mixture was stirred at room temperature for 1 h. To achieve highly homogeneous phosphor/silicone luminescent film, the mixture was vigorously mixed using a mechanical mixer. The YAG:Ce/silicone film was prepared by casting the final mixture, on a Teflon surface, by means of a coat-master 509MC-Erichsen (Dr Blade). The Dr Blade knife height was 1200 μm

dx.doi.org/10.1021/am404108n | ACS Appl. Mater. Interfaces 2014, 6, 252−258

and casting speed was 20 mm.s^{-1}. After having been casted, YAG:Ce/silicone film was allowed to dry on the Dr Blade plate for 15 min at 85 °C, then in an oven at 85 °C for 12 h. The measured final thickness of the film using a CADAR-MI20 was 830 μm.

Preparation of Bilayered YAG:Ce-CIS/ZnS QDs. The preparation of bilayered YAG:Ce-CIS/ZnS QDs was carried out in two steps. At first, YAG:Ce/silicone film was prepared according to the procedure described above. Second, CIS/ZnS-silicone mixture was cast on the surface of YAG:Ce/silicone film using Dr Blade method (Figure 1). CIS/ZnS-silicone mixture was prepared by mixing CIS/ZnS QDs suspension (0.2 g in chloroform) with 2.7 g of silicone resin. The chloroform solvent was then removed by heating at 85 °C. The final CIS/ZnS-silicone mixture was prepared by adding the curing agent to QD-silicone resin mixture. After it was dried in an oven at 85 °C for 12 h, the measured final thickness of the bilayered YAG:Ce-CIS/ZnS was 1200 μm.

Fabrication of YAG:Ce-CIS/ZnS QD-Based WLED Device. YAG:Ce-QD-based WLED was fabricated by combining 100 × 100 mm^2 InGaN-based blue LED (λ_{em} = 450 nm, non-epoxy molding packages, Optogan Co., Ltd.) with a bilayered YAG:Ce-CIS/ZnS QD film in remote configuration (Figure 1). Blue LED was connected to current regulator working in the range of 1−2 A and 1−30 V. The phosphor film and chip were separated by a reflector cup. The distance between phosphor film and chip was estimated to be 12 mm.

Characterization. The XRD measurements were performed using a Philips Xpert Pro diffractometer with Cu Kα radiation. Transmission Electron Microscopy (TEM) images were taken by placing a drop of the particles in solvent onto a carbon film-supported copper grid. Samples were studied using a Philips CM20 instrument operating at 200 kV. Scanning electron microscopy (SEM) images were recorded by means of a ZEISS Supra 55VP scanning electron microscope operating in high vacuum between 4 and 15 kV, using secondary electron detector (Everhart-Thornley detector). Specimens were prepared by sticking powder on the surface of an adhesive carbon film. Photoluminescence (PL) emission and excitation features as well as absolute photoluminescence quantum yield (QY) values were measured using a C9920-02G PL-QY measurement system from Hamamatsu. The setup comprises a 150 W monochromatized Xe lamp, an integrating sphere (Spectralon Coating, Ø = 3.3 in.) and a high sensitivity CCD spectrometer for detecting the whole spectral luminescence. Photoluminescence excitation (PLE) spectra were obtained by exciting the samples from 250 to 600 nm with 3 nm increment and measuring their absolute QY. Absolute QY values were then used and combined with the absorption coefficient (also measured by the apparatus) to plot the excitation spectra. Electroluminescent (EL) spectrum, luminous efficiency, CCT, Commission Internationale de l'Eclairage (CIE) color coordinates and CRI of the fabricated YAG:Ce and YAG:Ce-CIS/ZnS-based WLEDs were measured at room temperature under forward currents of 20, 40, 60, 80, 100, 120, 200, 400, 600, 800, 1000, and 1200 mA (corresponding to applied voltage of 7.6, 7.7, 7.8, 7.9, 8, 8.1, 8.2, 8.5, 8.7, 8.9, 9.1, and 9.3 V respectively) in an integrating sphere with a diode array rapid analyzer system (GL Optic integrating sphere GLS 500).

RESULTS AND DISCUSSION

The YAG:Ce nanocrystals and CIS/ZnS QDs were first characterized by XRD as shown in Figure 2. CIS/ZnS QDs exhibited three peaks of (112), (204)/(220), and (312)/(116) reflection planes (JCPDS Card N° 85−1575), which agree with the chalcopyrite phase of $CuInS_2$. In accordance with the literature,[34] the overcoating of CIS QDs with ZnS phase led to the overall shift of the reflection peaks to a larger 2θ values because of smaller lattice parameter of zinc blende ZnS (a = 0.5345 nm) compared to chalcopyrite $CuInS_2$ phase (a = 0.5517 nm). All diffraction peaks of as-prepared YAG:Ce NPs correspond to the pure $Y_3Al_5O_{12}$ phase (JCPDS file 88-2048) indicating that Ce^{3+} dopants were incorporated into the YAG host lattice without altering the original structure of YAG

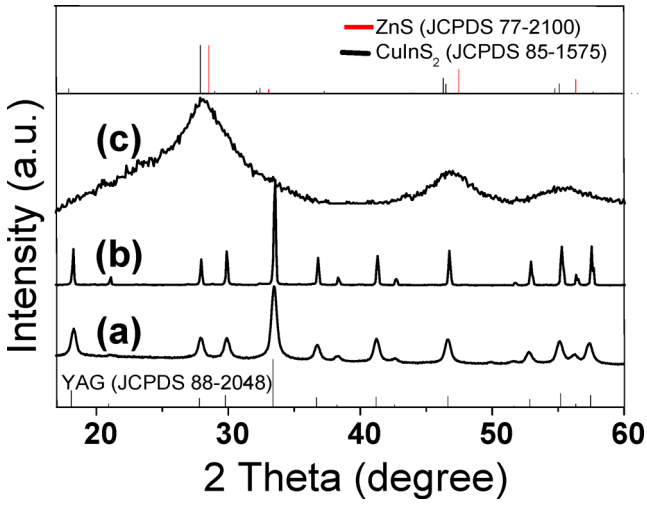

Figure 2. XRD patterns of (a) as-prepared YAG:Ce NPs, (b) 1500 °C-annealed YAG:Ce NPs, and (c) CIS/ZnS QDs.

(Figure 2a).[35] Broad peaks are consistent with the formation of YAG:Ce NPs as shown by TEM (see Supporting Information Figure S1). As expected, annealing of YAG:Ce NPs at 1500 °C leads to both an increase in diffraction intensity and a decrease in full-width at half-maximum (fwhm) because of the improvement of crystallinity, as well as the increase in crystallite size (Figure 2b). TEM and SEM images of annealed YAG:Ce nanocrystals and CIS/ZnS QDs are shown in Figure 3. TEM images of a representative CIS/ZnS QDs revealed the presence of well-dispersed monodisperse and spherical/ellipsoidal nanocrystals with an average diameter of 2.5 ± 0.3 nm (Figure 3a). The HR-TEM image of a single nanocrystal confirms the high crystallinity of CIS/ZnS QDs. SEM image of 1500 °C-annealed YAG:Ce NPs showed well-resolved and discernible nanophosphor particles with relatively large distribution of size and shape resulting from high temperature treatment (Figure 3b). From the SEM image, the particles size of 1500 °C-annealed YAG:Ce NPs was comprised between 100 and 300 nm.

Figure 4 shows PL excitation and emission spectra of YAG:Ce nanophosphor and CIS/ZnS QDs (see Supporting Information Figure S2 for the UV−vis absorption spectrum of the CIS/ZnS QDs). The PL emission spectrum of YAG:Ce nanophosphor consists of a broad band in the green-yellow range (maximum located around 545 nm). The emission is ascribed to the electron transitions from the lowest crystal-field splitting component of the 5d level to the ground state of Ce^{3+} (4f, $^2F_{5/2}$, $^2F_{7/2}$).[36] PLE spectrum showed two large bands having maxima located at 455 and 342 nm characteristic of YAG:Ce phosphor (Figure 4a). 1500 °C-annealed YAG:Ce NPs displayed higher QY of about 50%, upon 460 nm excitation, compared to their as-prepared counterpart (QY = 30%) mainly because of the improvement of crystallinity as shown by XRD patterns. Thermal treatment at 1500 °C could also promote the homogeneous incorporation of Ce^{3+} ions into the core of each YAG nanoparticle, which results in an increase in PL QY. The obtained CIS/ZnS QDs exhibited a large PL emission spectrum with a maximum located at 667 nm and a maximum PL quantum yield of 52% upon 460 nm excitation (Figure 4b). CIS/ZnS QDs also exhibited a large PLE spectrum ranging from UV to visible region. These optical features demonstrate that annealed solvothermally synthesized YAG:Ce nanophosphor and CIS/ZnS QDs are well suited to be

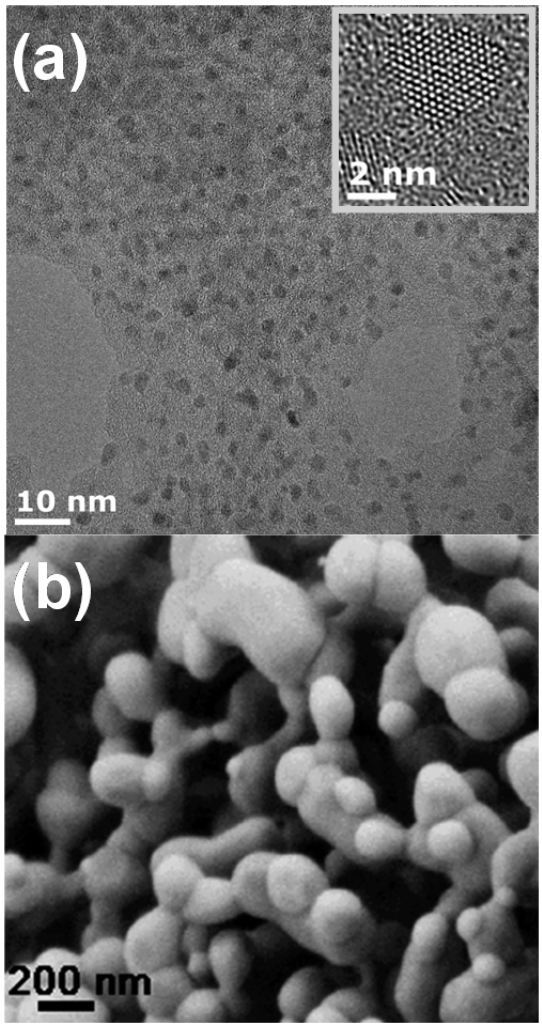

Figure 3. (a) TEM and HR-TEM images of CIS/ZnS QDs and (b) SEM image of 1500 °C-annealed solvothermally synthesized YAG:Ce NPs.

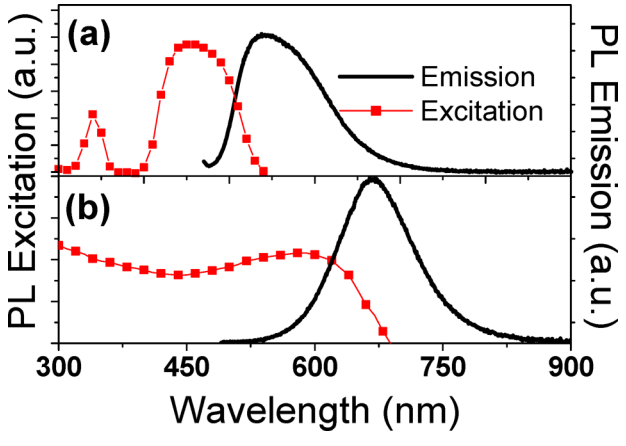

Figure 4. PL emission and excitation of (a) YAG:Ce nanophosphor and (b)CIS/ZnS core/shell QDs.

combined with GaN-based blue LEDs to convert blue light into warm white light.

Considering PL emission and excitation spectra, it seemed better to deposit CIS/ZnS QDs on YAG:Ce layer. Indeed, the spectral overlap between the phosphor emission and the absorption of the QDs indicates that photons emitted from the phosphor could definitely be absorbed and converted by the QDs. This phosphor-QDs energy transfer should be more important in the case of randomly mixed YAG:Ce/QDs in silicone resin (due to the increased optical interference between the QDs and YAG:Ce nanophosphor) thus increasing optical energy loss because of reabsorption and color conversion process. In the case of QDs layer on phosphor layer, most of blue light from InGaN chip is first efficiently converted by YAG:Ce phosphor. CIS/ZnS QDs then convert a part of blue light that are not absorbed by YAG:Ce (and possibly a part of blue-converted light transmitted through the phosphor layer) to generate red light. EL spectra of YAG:Ce and bilayered YAG:Ce-CIS/ZnS QDs-based WLED with increasing forward current from 20 to 1200 mA are shown in Figure 5. For annealed YAG:Ce NPs-based WLED, both blue and yellow emission increased in monotonic way without any saturation effect with increasing input current up to 1200 mA. Small change of CRI was observed (from 71 to 73) in this range of applied current. YAG:Ce nanophosphor-based WLED showed

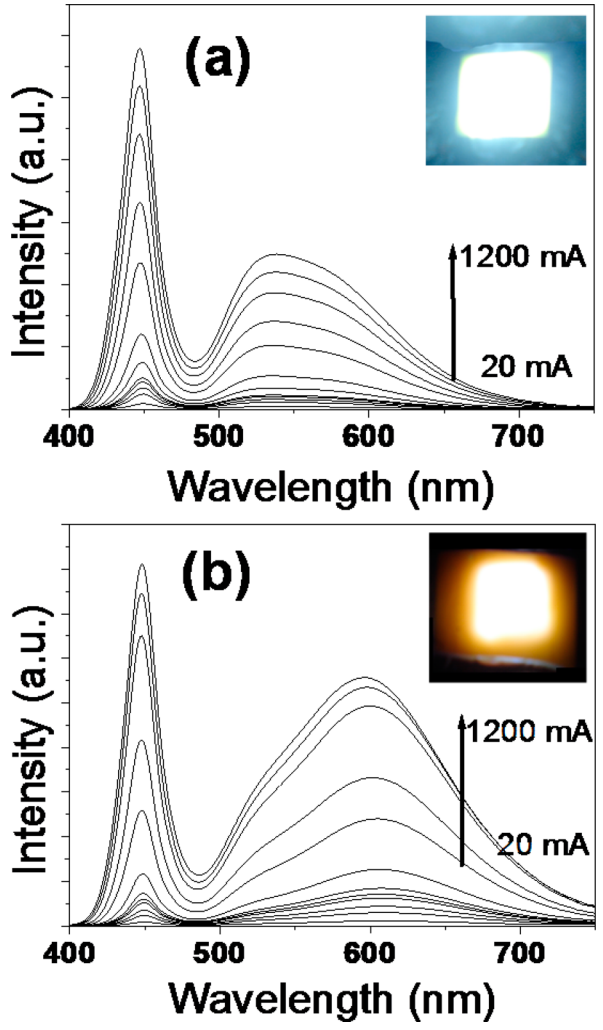

Figure 5. Evolution of EL spectra of (a) 1500-annealed YAG:Ce NPs and (b) bilayered YAG:Ce-CIS/ZnS QDs-based WLED with increasing forward current from 20 to 1200 mA. The photograph of the 1500-annealed YAG:Ce NPs and bilayered YAG:Ce-CIS/ZnS QDs-based WLED operated at 200 mA are shown in the inset of panels a and b, respectively.

dx.doi.org/10.1021/am404108n | ACS Appl. Mater. Interfaces 2014, 6, 252−258

limited color rendering property mainly due to the spectral deficiency of YAG:Ce in red region in agreement with the literature. CCT also increased from 7400 K at 20 mA to 9276 K at 1200 mA supported by a decrease in CIE color coordinates of x = 0.2966−0.2835, y = 0.3309−0.2970. Fabricated YAG:Ce-based WLED displayed cold and bluish white as shown in the inset of Figure 5a. As expected, bilayered YAG:Ce-CIS/ZnS QDs-based WLED displayed larger EL spectra since yellow and red emissions combine to generate the visible spectra. Compared to YAG:Ce-based WLED, EL spectra evolution of bilayered YAG:Ce-CIS/ZnS QDs-based WLED showed a beginning of saturation effect at high forward current (from 800 mA) indicating that CIS/ZnS QD emission would become saturated with increasing forward current up to 1200 mA. Saturation of CIS/ZnS QDs emission was already mentioned to explain the drop in light conversion efficiency with increasing current in pure CIS/ZnS QDs-based WLED up to 100 mA.[23] Indeed, CIS/ZnS QDs have considerably longer decay time of about 500 ns[37] compared to YAG:Ce phosphor (τ = 65 ns)[38] thus increasing the probability of PL saturation in QDs at high current density. Saturation of CIS/ZnS QDs emission is consistent with the blue-sided shift of EL spectra with increasing current and the increase in CCT from 2784 K at 20 mA to 3934 K at 1200 mA as shown in Figure 6a. This result is also consistent with a change in color coordinates (x = 0.43−0.36, y = 0.37−0.33) with increasing current. These observations could also be explained by thermal quenching of CIS/ZnS QDs at high current density due to a significant local heating of phosphor layer resulting from p−n junction temperature of InGaN chip. CRI parameter showed a very small change as a function of forward current from 20 to 1200 mA. High CRI of 84.6 was obtained at 1200 mA. These results indicated that white light generated from bilayered YAG:Ce NP-CIS/ZnS QDs-based WLED was relatively stable and warm white with high color rendering properties could be obtained regardless of applied current up to 1200 mA. Photograph of bilayered phosphor/QDs-based WLED is shown in the inset of Figure 5b. However, the luminous efficiency of bilayered phosphor-QDs-based WLED dropped rapidly from 30.6 to 21.1 lm W^{-1} in the 20−1200 mA range as shown in Figure 6b. The luminous efficiency of the bare InGaN blue chip used in this study was also measured in the same applied current conditions. Interestingly, the bare blue LED and bilayered phosphor/QDs-based WLED showed nearly the same efficiency drop of 29.5% and 31%, respectively, in 20−1200 mA range suggesting that the observed decrease in luminous efficiency is ascribed to the intrinsic efficiency drop of the blue LED chip itself. We also studied the evolution of the CRI and CCT of bilayered YAG:Ce-CIS/ZnS QDs-based WLED operated at 200 mA with increasing operating time (Figure 7). Both CRI and CCT curves showed a rapid change in the first seven hours; CRI dropped from 82.1 to 80.1, while CCT rose from 2950 to 3450 K after 7 h of WLED operation at 200 mA. These results are consistent with a blue-sided shift of EL spectra (see Supporting Information Figure S3) throughout the first seven hours of WLED operation. These changes are closely related to the higher thermal quenching of CIS/ZnS QDs than that of YAG:Ce nanophosphor (see Supporting Information Figure S4). We found that the highest temperature of CIS/ZnS QDs layer can reach 40 °C with applied current of 200 mA (operating conditions of Figure 7). At this temperature, while the PL QY of YAG:Ce nanophosphor remained almost unchanged, PL QY loss by thermal quenching of CIS/ZnS QDs is about 10% thus indicating that the rapid CCT and CRI changes observed in the first 7 h are mostly caused by thermal quenching of CIS/ZnS QDs. With extending operating time to t > 7 h, CRI and CCT progressively tend to stabilize at 80 and 3660 K, respectively. At t > 7 h, emission wavelength of EL spectra remained almost unchanged throughout the 33 h operation period (Supporting Information Figure S3). The initial YAG:Ce-CIS/ZnS QD emission intensity also remained almost unchanged throughout the 40 h operation period. As a natural consequence, the luminous efficiency was nearly constant (26 lm W^{-1}) irrespective of the operating time. These first results are very promising and demonstrate that

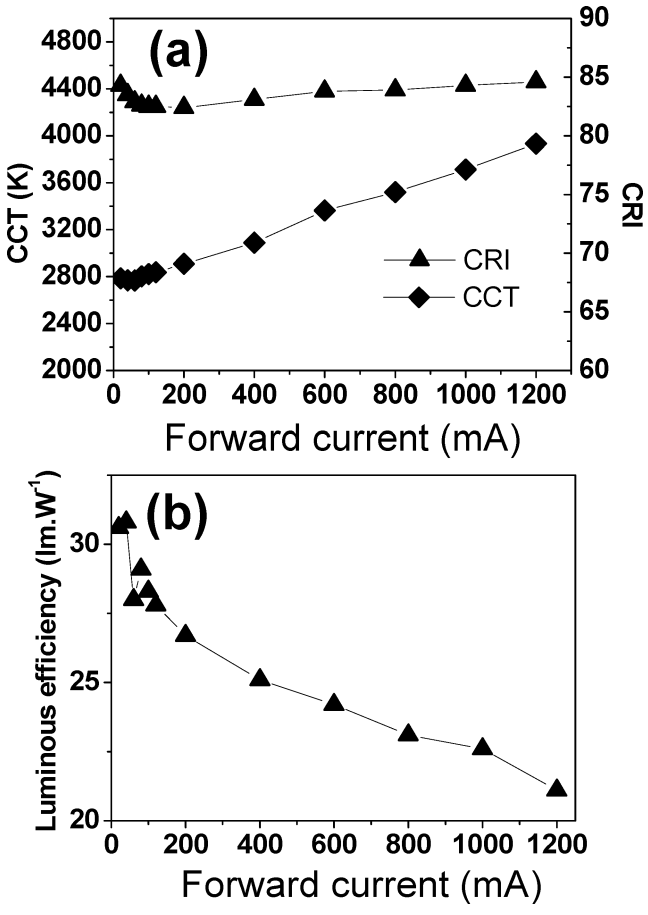

Figure 6. Variation of (a) CCT and CRI and (b) luminous efficiency of bilayered YAG:Ce-CIS/ZnS QDs-based WLED with increasing forward current from 20 to 1200 mA.

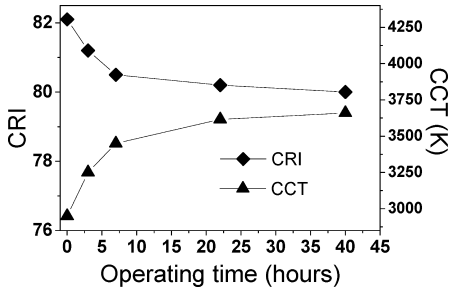

Figure 7. Temporal evolution of the CRI and CCT of bilayered YAG:Ce-CIS/ZnS QDs-based WLED operated at 200 mA for a prolonged duration up to 40 h.

dx.doi.org/10.1021/am404108n | ACS Appl. Mater. Interfaces 2014, 6, 252−258

using phosphor-red emitting CIS/ZnS QDs bilayered converter film we could be able to get relatively stable warm white light with high CRI even at high input current of 200 mA. Experiments are in progress to study longer operating time effect on the stability of white light generated from bilayered YAG:Ce phosphor-red QDs-based WLED and improve the quality and stability of warm white light during LED operation.

CONCLUSION

YAG:Ce nanocrystals with a particle size comprised between 100 and 300 nm were successfully prepared by annealing solvothermally synthesized YAG:Ce NPs at 1500 °C without H_2 reducing gas. These nanocrystals and red emitting CIS/ZnS core/shell QDs were successfully combined with a blue InGaN LED to achieve warm white light possessing high CRI of about 84. This high CRI was attained by compensating the red spectral deficiency of YAG:Ce nanophosphor by a red emission of CIS/ZnS QDs. QDs on YAG:Ce nanocrystals bilayered structure was prepared by casting CIS/ZnS QDs-silicone mixture on the surface of YAG:Ce-silicone film and applied to blue LED chip in remote phosphor configuration. Bilayered YAG:Ce nanocrystals-red emitting QDs-based-WLED showed a CCT rise from 2784 to 3934 K and a luminous efficiency drop from 30.6 to 21.1 lm W^{-1} with increasing applied current from 20 to 1200 mA. We demonstrated that the fall in luminous efficiency is a consequence of the intrinsic efficiency drop of the blue LED chip. The YAG:Ce-red emitting CIS/ZnS QDs-based WLED displayed an interesting device stability with extending operating time up to 40 h with applied current of 200 mA. Although CRI and CCT of such device change rapidly during the first seven hours of operating (82−80 and 2950−3450 K, respectively), CRI and CCT tend to remain constant from 7 to 40 h thereafter. The luminous efficiency was also nearly constant (26 lm.W^{-1}) irrespective of the operating time. This result suggests that QDs on phosphor bilayered structure could provide a simple and suitable way to stable white light quality from WLED with extending operating time. This way also provides a simple solution to predict and adjust light properties from WLED by varying only the thickness of phosphor or QDs layer.

ASSOCIATED CONTENT

Supporting Information

TEM image of the as-prepared YAG:Ce NPs, absorption spectrum of CIS/ZnS core/shell QDs, temporal evolution of EL spectra of bilayered YAG:Ce-CIS/ZnS QDs-based WLED operated at 200 mA for a prolonged duration up to 40 h and temperature dependence of relative PL QY of YAG:Ce nanophosphor and CIS/ZnS QDs. This information is available free of charge via the Internet at http://pubs.acs.org/.

AUTHOR INFORMATION

Corresponding Author

*E-mail: a.abdelhay@hotmail.com. Fax: +33(0)4 73 40 71 08. Tel: +33 (0) 4 73 40 76 07.

Notes

The authors declare no competing financial interest.

ACKNOWLEDGMENTS

The authors thank "Clermont-Communauté" for financial support and Christelle Blavignac (CICS, Université d'Auvergne, France) for TEM observations.

REFERENCES

(1) Shionoya, S. *Phosphor Handbook*; CRC Press: Boca Raton, FL, 1998.
(2) Blasse, G. *J. Alloys Compd.* **1995**, *225*, 529−533.
(3) Bachmann, V.; Ronda, C.; Oeckler, O.; Schnick, W.; Meijerink, A. *Chem. Mater.* **2008**, *21*, 316−325.
(4) Jang, H. S.; Yang, H.; Kim, S. W.; Han, J. Y.; Lee, S.-G.; Jeon, D. Y. *Adv. Mater.* **2008**, *20*, 2696−2702.
(5) Setlur, A. A.; Heward, W. J.; Hannah, M. E.; Happek, U. *Chem. Mater.* **2008**, *20*, 6277−6283.
(6) Schlotter, P.; Schmidt, R.; Schneider, J. *Appl. Phys. A: Mater. Sci. Process.* **1997**, *64*, 417−418.
(7) Jang, H.; Won, Y. H.; Jeon, D. *Appl. Phys. B: Lasers Opt.* **2009**, *95*, 715−720.
(8) Jang, H.; Im, W.; Lee, D.; Jeon, D.; Kim, S. *J. Lumin.* **2007**, *126*, 371−377.
(9) Wang, L.; Zhang, X.; Hao, Z. D.; Luo, Y. S.; Wang, X. J.; Zhang, J. H. *Opt. Express* **2010**, *18*, 25177−25182.
(10) Yang, H.; Kim, K. *J. Lumin.* **2008**, *128*, 1570−1576.
(11) Wang, W. D.; Tang, J. K.; Hsu, S. T.; Wang, J.; Sullivan, B. P. *Chem. Phys. Lett.* **2008**, *457*, 103−105.
(12) Shi, Y.; Wang, Y.; Wen, Y.; Zhao, Z.; Liu, B.; Yang, Z. *Opt. Express* **2012**, *20*, 21656−21664.
(13) Pan, Y. X.; Wu, M. M.; Su, Q. *J. Phys. Chem. Solids* **2004**, *65*, 845−850.
(14) Katelnikovas, A.; Bettentrup, H.; Uhlich, D.; Sakirzanovas, S.; Justel, T.; Kareiva, A. *J. Lumin.* **2009**, *129*, 1356−1361.
(15) Ye, S.; Xiao, F.; Pan, Y. X.; Ma, Y. Y.; Zhang, Q. Y. *Mater. Sci. Eng., R* **2010**, *71*, 1−34.
(16) Ooyabu, Y.; Nakamura, T.; Fuji, H.; Ito, H. Light-Emitting Device. U.S. Patent 2012/0032219 A1, February, 9, 2012.
(17) Dai, Q.; Duty, C.-E.; Hu, M.-Z. *Small* **2010**, *6*, 1577−1588.
(18) Anc, M. J.; Pickett, N. L.; Gresty, N. C.; Harris, J. A.; Mishra, K. C. *ECS J. Solid State Sci. Technol.* **2013**, *2*, 3071−3082.
(19) Kim, K.; Jeong, S.; Woo, J.−Y.; Han, C.-S. *Nanotechnology* **2012**, *23*, 065602−065608.
(20) Menkara, H.; Gilstrap, R. A., Jr.; Morris, T.; Minkara, M.; Wagner, B. K.; Summers, C. J. *Opt. Express* **2011**, *19*, A972−A981.
(21) Aboulaich, A.; Billaud, D.; Abyan, M.; Balan, L.; Gaumet, J.-J.; Medjadhi, G.; Ghanbaja, J.; Schneider, R. *ACS Appl. Mater. Interfaces* **2012**, *4*, 2561−2569.
(22) Kim, H.; Han, J.-Y.; Kang, D.-S.; Kim, S.-W.; Jang, D.-S.; Suh, M.; Kirakosyan, A.; Jeon, D.-Y. *J. Cryst. Growth* **2011**, *326*, 90−93.
(23) Song, W.-S.; Yang, H. *Chem. Mater.* **2012**, *24*, 1961−1967.
(24) Song, W.-S.; Kim, J.-H.; Lee, J.-H.; Lee, H.-S.; Jang, H.-S.; Yang, H. *Mater. Lett.* **2013**, *92*, 325−329.
(25) Song, W.-S.; Jang, E.-P.; Kim, J.-H.; Jang, H.-S.; Yang, H. *J. Nanopart. Res.* **2013**, *15*, 1462−1472.
(26) Kim, S.; Kim, T.; Kang, M.; Kwak, S. K.; Yoo, T. W.; Park, L. S.; Yang, I.; Hwang, S.; Lee, J. E.; Kim, S. K.; Kim, S.-W. *J. Am. Chem. Soc.* **2012**, *134*, 3804−3809.
(27) Aboulaich, A.; Geszke, M.; Balan, L.; Ghanbaja, J.; Medjahdi, G.; Schneider, R. *Inorg. Chem.* **2010**, *49*, 10940−10948.
(28) Song, W.-S.; Nam, D.-E.; Yang, H. *J. Nanoelectron. Optoelectron.* **2011**, *6*, 234−238.
(29) Chen, B.; Zhou, Q.; Li, J.; Zhang, F.; Liu, R.; Zhong, H.; Zou, B. *Opt. Express* **2013**, *21*, 10105−10110.
(30) Pradal, N.; Chadeyron, G.; Potdevin, A.; Deschamps, J.; Mahiou, R. *J. Eur. Ceram. Soc.* **2011**, *6*, 234−238.
(31) Liu, Z.; Liu, S.; Wang, K.; Luo, X. *Front. Optoelectron. China* **2009**, *2*, 119−140.
(32) Park, S.-C.; Rhee, I.; Kim, J.-Y.; Bark, H. J.; Jeong, J. *J. Korean Phys. Soc.* **2012**, *60*, 1191−1195.
(33) You, J. P.; Tran, N. T.; Shi, F. G. *Opt. Express* **2010**, *18*, 5055−5060.
(34) Nam, D.-E.; Song, W.-S.; Yang, H. *J. Colloid Interface Sci.* **2011**, *361*, 491−496.

(35) Aboulaich, A.; Deschamps, J.; Deloncle, R.; Potdevin, A.; Devouard, B.; Chadeyron, G.; Mahiou, R. *New J. Chem.* **2012**, *36*, 2493−2500.
(36) Blasse, G.; Grabmaier, B. C. *Luminescent Materials*; Springer-Verlag: Berlin, 1994; pp 45−46.
(37) Shi, A.; Wang, X.; Meng, X.; Liu, X.; Li, H.; Zhao, J. *J. Lumin.* **2012**, *132*, 1819−1823.
(38) Bachmann, V.; Ronda, C.; Meijerink, A. *Chem. Mater.* **2009**, *21*, 2077−2084.